Lattice dynamics of berlinite ($AlPO_4$): a comparative study with quartz (SiO_2)

1994 J. Phys.: Condens. Matter 6 5351

(http://iopscience.iop.org/0953-8984/6/28/011)

J. Phys.: Condens. Matter 6 (1994) 5351–5372. Printed in the UK

Lattice dynamics of berlinite ($AlPO_4$): a comparative study with quartz (SiO_2)

H Schober†‡ and B Dorner§

† Kernforschungszentrum Karlsruhe, D-76021 Karlsruhe, Germany
‡ DRFMC-SPSMS-MDN, CENG, 38054 Grenoble Cedex 9, France
§ Institut Laue–Langevin, F-38042 Grenoble, France

Received 10 March 1994

Abstract. We present model calculations for the lattice dynamics of berlinite ($AlPO_4$). The short-range potentials used for the calculation are based on the ones determined for quartz (SiO_2). The polarizability of the oxygen ion is taken into account by an adiabatically moving shell. A good description both of the experimental frequencies and the high-frequency dielectric constants is obtained. Estimates of the ionic as well as effective charges of the constituent ions are given. The deduced charges in conjunction with the obtained polarizability indicate a similar charge state of the oxygen ion in quartz and berlinite. The ionic charges of phosphorus and aluminium differ strongly. The same observation is made for the short-range forces between the cations and oxygen. On the basis of these results the picture of an oxygen framework crystal is discarded. Special effort is devoted to the investigation of equilibrium conditions. The stability of the respective tetrahedra turns out to be of central importance for the dynamics of both quartz and berlinite. Consequences for the α- to β-phase transition are discussed.

1. Introduction

Besides its potential for technical applications (see Jayaraman *et al* 1987, Sidek *et al* 1987), which mainly relies on its favourable piezoelectric properties, berlinite ($AlPO_4$) is of fundamental interest for understanding the bonding of tetrahedrally coordinated oxides in general. This interest has received new impetus due to the memory phenomenon berlinite exhibits in connection with order–disorder transitions under pressure (see Kruger *et al* 1990, Chelikowsky *et al* 1990).

Starting with the early structural work of Schwarzenbach (1966) one of the central questions raised in connection with berlinite is whether it should be regarded as $(AlP)O_4$, i.e. a framework crystal, or as an ionic structure of the type $Al^{3+}(PO_4)^{3-}$. While the diffuse x-ray scattering intensities support an ionic structure (see Schwarzenbach 1966), it is, in particular, the similarities shared by berlinite and quartz (SiO_2) which point towards a framework crystal. These similarities are not limited to a common structure (see section 2), but extend as well to the dynamics of the crystals (see Bethke *et al* 1992). Even the well known transition from the α- to the β-phase, observed in quartz, is not only present in berlinite, but also takes place at nearly the same temperature ($T_c \approx 857$ K in $AlPO_4$ and $T_c \approx 846$ K in SiO_2).

Given these similarities the question of the binding in berlinite can be answered best by carrying out a comparative study with quartz. Such a study is made possible by the fact that both for berlinite and for quartz sufficient experimental data are available. While the determination of the phonon dispersion in quartz has been a subject of continuing research

0953-8984/94/285351+22$19.50

for many years (for an overview see Strauch and Dorner 1993) accurate experimental data for the phonon frequencies in berlinite are rather recent (Scott 1971, Camassel *et al* 1988, Bethke *et al* 1992).

To our knowledge, there have been two major attempts to describe the lattice dynamics of berlinite (Bethke *et al* 1992, Scott 1971). Both of them neglect the polarizability of the oxygen ion. Scott (1971) comes to the conclusion that there is a strong charge compensation in berlinite ($Z_{Al} - Z_P \leqslant 0.2\epsilon^{\infty}e$). Bethke *et al* go one step further and interpret their results in terms of an oxygen framework crystal. Including the polarizability of the oxygen ion, we will give a different picture of the bonding in berlinite and show that this picture is compatible with the experimental results.

We start our investigation by employing lattice-dynamical shell models developed for quartz to describe the lattice dynamics of berlinite (for a general description of lattice-dynamical models see e.g. Sinha 1973 and references therein). Although desirable, a perfect description of the experimental frequencies in berlinite is not the ultimate objective of our study. Instead, we want to keep the changes within the models as small as possible while at the same time achieving a satisfactory reproduction of the experimental data. This way we obtain valuable information on the essential changes in the charge states and bonding accompanying the substitution of silicon by aluminum and phosphorus. As in quartz it will turn out that, in order to achieve an understanding of the dynamics, it is advantageous to include the study of the dielectrical properties of the crystal.

The paper is structured as follows. In section 2 we give a short description of the structure of berlinite followed by a summary of the experimental data in section 3. The lattice-dynamical models will be presented in section 4 while section 5 deals in detail with charges and polarizabilities. Section 6 is concerned with crystal equilibrium and section 7 treats the temperature dependence of the phonon spectrum.

2. Structure

Berlinite ($AlPO_4$) consists of a three-dimensional alternation of slightly deformed AlO_4 and PO_4 tetrahedra which are linked at the corners by common oxygen ions (see figure 1). Like quartz low-temperature berlinite exists in two species known as Dauphiné twins. The left- and right-handed modifications of these species belong, respectively, to the space groups $P3_121$ (D_3^4) and $P3_221$ (D_3^6). There is a transition at approximately 857 K to the high-temperature phase. Unless explicitly stated berlinite in this work denotes the low-temperature phase otherwise known as α-berlinite and the same convention applies to quartz.

A detailed description of the structure which is defined by two lattice constants and eight structural parameters is given by Schwarzenbach (1966) and Ng and Calvo (1976). In this work we will use, unless stated otherwise, the structural parameters of Schwarzenbach (1966). The coordinates of the atoms are given in table 1 for reference.

The average distance between phosphorus and neighbouring oxygen ions being 1.516 Å the PO_4 tetrahedra† are appreciably smaller than the AlO_4 tetrahedra with an average

† These values are very close to the ones found in other materials for the distances within $(PO_4)^{3-}$ tetrahedra. E.g. r(P–O) is approximately 1.54 Å in fluorapatite ($Ca_{10}(PO_4)_6F_2$) (Boyer and Fleury 1974) and hydroxyapatite ($Ca_{10}(PO_4)_6F_2$) (Posner *et al* 1958). As the molecular-crystal character of these substances is well established this observation should be taken into account when discussing the character of the binding in berlinite. See also the paper by Averbuch-Pouchot (1993) and references therein for bond lengths within PO_3H tetrahedra in organic phosphites.

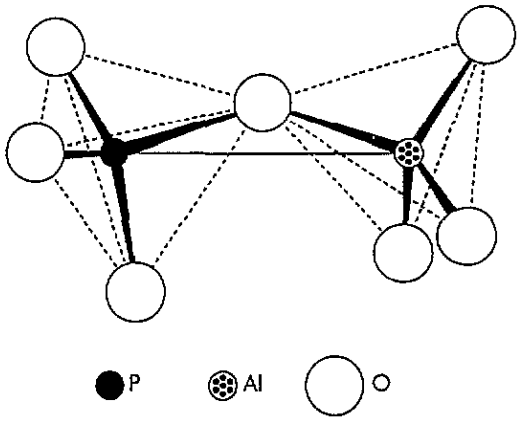

Figure 1. Schematic view of the binding in berlinite (taken from Bethke *et al* 1992). Open circles: oxygen ions; full circles: phosphorus ions; dotted circles: aluminium ions. The AlO_4 tetrahedra share common oxygen ions with the PO_4 tetrahedra.

Table 1. Cartesian coordinates of the atomic positions in α-berlinite using the structural parameters of Schwarzenbach (1966). Units are Å. a_1, a_2 and a_3 are the hexagonal Bravais vectors.

No	x	y	z
a_1	4.9429	0.0000	0.0000
a_2	−2.4715	4.2807	0.0000
a_3	0.0000	0.0000	10.9476
1 (Al)	2.3054	0.0000	3.6492
2 (Al)	−1.1527	1.9965	−3.6492
3 (Al)	−1.1527	−1.9965	0.0000
4 (P)	2.3078	0.0000	−1.8246
5 (P)	−1.1540	1.9987	1.8246
6 (P)	−1.1540	−1.9987	5.4738
7 (O)	1.3376	1.2491	4.3593
8 (O)	0.4130	1.7829	−4.3593
9 (O)	−1.7505	0.5338	−2.9391
10 (O)	−1.7505	−0.5338	−0.7101
11 (O)	0.4130	−1.7829	0.7101
12 (O)	1.3376	−1.2491	2.9391
13 (O)	1.4258	1.0998	−1.2780
14 (O)	0.2395	1.7847	1.2776
15 (O)	−1.6653	0.6849	2.3716
16 (O)	−1.6653	−0.6849	4.9268
17 (O)	0.2395	−1.7847	−4.9268
18 (O)	1.4258	−1.0998	−2.3716

aluminium–oxygen nearest-neighbour distance of 1.739 Å. For the following discussion it is essential to know that berlinite can be built up from quartz by replacing the silicon ions alternately by phosphorus and aluminium while simultaneously making small corrections to the bond lengths. In order to facilitate the comparison we have listed the atomic distances up to ~ 3 Å for both structures in table 2.

A very detailed description of the symmetry properties of berlinite including phonon representations and their selection rules is given by Bethke *et al* (1992) and will not be repeated here.

3. Experimental data

The vibrational spectrum of berlinite has been investigated both by optical spectroscopy and

Table 2. Nearest-neighbour distances in α-berlinite. The values for α-quartz are given for comparison. The numbering is consistent with table 1 for berlinite and the article by Schober *et al* (1993) for quartz.

No	Ion pair	r_{ik} (Å)	No	Ion pair	r_{ik} (Å)
1	Al(1)–O(7)	1.7324	1	Si(1)–O(4)	1.6079
2	Al(1)–O(15)	1.7455	2	Si(1)–O(6)	1.6100
3	P(4)–O(13)	1.5122			
4	P(4)–O(9)	1.5197			
5	O(13)–O(18)	2.4565	3	O(4)–O(7)	2.6154
6	O(7)–O(8)	2.4714	4	O(4)–O(9)	2.6161
7	O(7)–O(16)	2.4721	5	O(4)–O(5)	2.6282
8	O(7)–O(17)	2.4903	6	O(4)–O(6)	2.6444
9	O(7)–O(16)	2.7976			
10	O(7)–O(15)	2.8343			
11	O(7)–O(12)	2.8737			
12	O(13)–O(14)	2.8995			
13	Al(1)-P(5)	3.0843	7	Si(1)–Si(2)	3.0572
14	Al(1)-P(5)	3.0862			

inelastic neutron scattering. Although optical spectroscopy is limited to long wavelengths, the frequencies thus obtained are of special importance to the present investigation as they cover the whole frequency range of the vibrational spectrum up to 40 THz. The neutron data available so far (Bethke *et al* 1992) are limited to energies below 8 THz. An extensive study of the infrared activity of berlinite has been carried out by Camassel *et al* (1985). An analysis of the Raman spectra has been done by Scott (1971). The modes at the zone centre belong to three irreducible representations which are denoted Γ_1, Γ_2 and Γ_3. The eight optical modes of representation Γ_1 are Raman active, only, while the nine optical modes of representation Γ_2 are infrared active, only. Representation Γ_3 is twofold degenerate and its 2×17 optical modes are both Raman and infrared active. A very interesting discussion of the changes in optical activity when going from β-quartz to α-quartz and then to α-berlinite is given by Camassel *et al* (1988). In the latter article one also finds a comparison of the results obtained by different experimental groups. The agreement is generally quite good. There is, however, one strong discrepancy for two frequencies of the Γ_3 representation. Scott (1971) claims to observe in his Raman spectra a polar mode at $\nu_{TO} = 13.8$ THz and $\nu_{LO} = 17.0$ THz respectively which according to Camassel *et al* (1988) shows up at $\nu_{TO} = 14.2$ THz and $\nu_{LO} = 15.7$ THz in the infrared reflectivity data. This discrepancy will become important in section 5 when we are dealing with the LO–TO splitting in berlinite. The numerical values for the optical frequencies used in this work are summarized in table 3.

An extensive study of the lower-lying ($\nu < 8$ THz) dispersion branches of berlinite by inelastic neutron scattering has been carried out by Bethke *et al* (1992). As we will not explicitly adjust, but only compare our models to the neutron data, we do not reproduce the numerical values for the frequencies but refer the reader to the original publication. The neutron data are nevertheless of fundamental importance to our study as they allow us to check the predictions of our models in the interior of the Brillouin zone.

As discussed by Bethke *et al* the dispersion relations of berlinite in the Γ–A direction, i.e. along the threefold axis, can be interpreted in terms of a back-folding of the dispersion relations found for quartz. This back-folding is due to the doubling of the primitive cell along the threefold axis when going from the quartz to the berlinite structure. If we extend this observation, which has been made for the lower-frequency spectrum, to all vibrations then the Γ-point modes in berlinite contain already the information of the Γ- plus A-point modes in quartz. Fitting the models only to the optical frequencies, therefore, seems to be

Table 3. Optical frequencies at the Γ point for berlinite in terahertz. The experimental frequencies listed in columns 2 and 3 are taken from the Raman measurements of Scott (1971) for the Γ_1 representation and from the infrared reflectivity measurements of Camassel *et al* (1988) for the Γ_2 and Γ_3 representations. The theoretical predictions of the shell models SM(2) and SM(3) are given in columns 4 and 5 and 6 and 7, respectively. The model parameters can be found in table 4.

IMR	LO_{exp}	TO_{exp}	LO(SM(2))	TO(SM(2))	LO(SM(3))	TO(SM(3))
Γ_1	4.7		5.8		4.9	
	6.5		6.5		6.4	
	10.1		9.4		10.0	
	—		11.0		12.3	
	13.7		12.4		13.6	
	21.9		20.8		20.7	
	33.2		33.1		32.4	
	33.5		33.9		33.7	
Γ_2	1.4	1.4	1.7	1.7	1.5	1.5
	4.2	4.2	4.0	4.0	3.6	3.6
	8.2	8.1	8.6	8.4	7.2	6.9
	13.4	13.2	13.8	13.7	13.9	13.8
	16.3	14.7	16.2	14.6	16.1	15.5
	21.1	20.5	21.3	20.8	21.5	21.3
	—	—	22.9	22.6	22.9	22.9
	34.8	34.8	33.7	32.7	34.2	33.5
	36.9	32.8	38.6	34.3	37.9	34.8
Γ_3	3.4	3.4	2.8	2.8	3.0	3.0
	3.8	3.8	3.4	3.4	3.4	3.2
	5.0	5.0	5.4	5.4	5.1	5.1
	6.2	5.9	6.2	6.2	6.1	6.1
	8.6	8.5	8.6	8.6	9.4	9.3
	—	—	11.0	10.9	12.1	12.0
	11.5	11.4	11.7	11.7	12.1	12.1
	12.4	12.4	12.3	12.3	13.1	13.1
	15.7	14.2	15.5	13.4	14.5	13.9
	—	—	17.3	17.3	17.1	17.0
	19.5	19.5	20.3	19.7	19.5	19.4
	21.7	21.3	21.5	21.3	21.0	20.7
	22.1	22.1	23.8	23.5	22.8	22.8
	33.7	33.0	33.9	33.0	32.9	32.8
	35.4	33.9	34.0	34.1	34.3	33.9
	36.8	35.4	38.1	34.7	37.4	34.8
	37.2	36.8	39.0	38.5	38.2	37.7

an adequate choice.

4. Model calculations

To our knowledge, all theoretical approaches dealing with the lattice dynamics of berlinite so far have been based on phenomenological models of the Born–von Kármán or rigid-ion type (Bethke *et al* 1992, Scott 1971). Due to the very effective screening of the long-range forces this procedure seems legitimate as long as one concentrates on the low-frequency part of the spectrum. The description of the experimental frequencies achieved by Bethke *et al* (1992) using a simple five-parameter Born–von Kármán model is impressive.

In the case of α-quartz (SiO_2) (Schober *et al* 1993) we had found that, although the lower part of the dispersion branches may be described very well by simple short-range models (see Barron *et al* 1976), the polarizability of the oxygen ion has to be taken into consideration in order to achieve an overall understanding of the lattice dynamics of the crystal. As quartz (SiO_2) and berlinite ($AlPO_4$), both structurally and chemically, are very similar it is to be expected that this also holds for the latter.

We start our investigations with the shell model SM(1) which has given very satisfactory results for quartz. Model SM(1) is a shell model with short-range interactions specified among oxygen shells as well as between oxygen shells and silicon cores†. The short-range interactions are in both cases derived from Born–Mayer potentials (see equation (1)) thus limiting the number of free parameters.

$$V(r) = V_0 \exp(-r/a). \tag{1}$$

It turns out that in order to achieve a good description of the acoustic branches in quartz one has to add small valence forces which we choose to be of the Keating type (1966):

$$V_{\text{Keating}} = -\sum_{ii'i''} \beta_{i'ii''} \frac{[\boldsymbol{r}_{ii'} \cdot \boldsymbol{r}_{ii''} - \beta'_{i'ii''} \boldsymbol{r}^0_{ii'} \cdot \boldsymbol{r}^0_{ii''}]^2}{\boldsymbol{r}^0_{ii'} \cdot \boldsymbol{r}^0_{ii''}}. \tag{2}$$

Here, $\boldsymbol{r}_{ii'}$ is the vector pointing from particle i to particle i', and the superscript 0 denotes the equilibrium positions. The Keating forces are necessary both for the inter-tetrahedral (Si–O–Si) as well as the intra-tetrahedral angles (O–Si–O).

The charge of the oxygen ion is not a free parameter in model SM(1) but fixed at the nominal value of $-2e$. The parameter values of the model are given in table 4. For a more detailed description of the model see the article by Schober *et al* (1993).

Model SM(1) can be applied straightforwardly to berlinite. The only additional parameter necessary is the one determining the distribution of the positive charge — which in quartz is concentrated on the silicon ions — among the phosphorus and aluminium cations. In a first, simplified approach we choose the ionic charges to have the nominal values of the respective valences, i.e. $3e$ for the aluminium and $5e$ for the phosphorus ion. As we have *a priori* no reason to believe that the inter-tetrahedral valence forces in quartz are the same as the ones in berlinite we include at this early stage neither Keating potentials for the Al–O–P angles nor a direct Al–P interaction. As we still expect strong intra-tetrahedral forces to arise from the sp^3 hybridization of the phosphorus orbitals, however, we keep the Keating potentials—obtained for the O–Si–O angles in quartz—for the O–P–O angles in berlinite. If we compare the frequencies for the zone centre modes calculated by such a model with the experimental values we realize that, although the crystal is stable, the agreement is not very good. It turns out that in order to improve the description of the experimental data it is sufficient to reduce the amplitude of the P–O potential slightly (about 10%) while retaining the value of the Si–O potential for the Al–O potential. In addition, we have to adjust one of the Keating parameters to the experimental data (see table 3). The Γ-point frequencies calculated with this model—which we call SM(2)—are listed in table 3. The parameter values are given in table 4. Considering the fact that out of the 10 free parameters of the model only two have been adjusted to the data, while the rest have been transferred

† For numerical reasons we have chosen a small polarizability ($\alpha = 0.03$ Å^3) and large shell charge ($Y = -8e$) for the cations. Thus, although the interactions are actually specified between cation and oxygen shells, they effectively act between cation cores and oxygen shells.

Table 4. Parameters of the shell models SM(1) and SM(4) for quartz and SM(2) and SM(3) for berlinite. The interactions are numbered according to table 2. Z is the ionic charge, Y the shell charge, and α the free-oxygen polarizability. L and T denote longitudinal and transverse force constants. V and a are the amplitude and decay constant of the Born–Mayer potentials, see equation (1). β and β' are the Keating parameters, see equation (2). The subscripts inter and intra stand for the inter-tetrahedral and intra-tetrahedral angles, respectively. In the case of berlinite the intra-tetrahedral interactions are confined to the O–P–O angles. All Keating interactions act between cores only. The values in parenthesis apply to model SM(4) with direct silicon–silicon interactions. Parameters marked by an asterisk have been kept fixed. For models SM(2) and SM(3) $\Delta\nu$ is the mean square deviation of the calculated frequencies from the experimental frequencies in table 3. In the case of models SM(1) and SM(4) $\Delta\nu$ is defined as in the article by Schober *et al* (1993). n_p is the number of free model parameters.

Interaction	No	SM(1)	SM(4)	No	SM(2)	SM(3)	Unit
V	1,2	7800	7275	1,2	7800	7275	eV
a	1,2	0.2089	0.2039	1,2	0.2089	0.2039	Å
V				3,4	7320	7275	eV
a				3,4	0.2089	0.2039	Å
V	3–6	240		7–12	240		eV
a	3–6	0.430		7–12	0.430		Å
L	7	−128	(−80)				N m^{-1}
T	7	−12	(2)				N m^{-1}
Z_O		−2.00*	−1.68		−2.00*	−1.68	e
Z_P					5.00*	4.51	e
Y(O)		−3.13	−3.03		−3.13	−3.03	e
α(O)		1.86	1.73		1.86	1.73	Å^3
β_{inter}		5.2	1.6 (5.1)			16.8	N m^{-1}
β'_{inter}		1.0	4.2 (2.5)			1.3	
β_{intra}		1.5	3.3 (3.3)		1.5	6.7	N m^{-1}
β'_{intra}		2.2	2.0 (2.4)		6.5	1.5	
n_p		12	9		10	10	
$\Delta\nu$		0.31	0.66		0.70	0.55	THz

unchanged from model SM(1) of quartz, the agreement with experiment is very good (see table 3). This good agreement is the more surprising as both the Coulomb interactions and the short-range force constants have changed dramatically when going from quartz to berlinite. The change in the Coulomb interactions is due to the unequal distribution of the positive charge among the cations of berlinite while the differences in the bond lengths (see table 2) are responsible for the changes in the short-range force constants. As we want to emphasize this point we have listed in table 5 the force constants derived from the Coulomb as well as Born–Mayer potentials for the anion–cation interactions of both quartz and berlinite.

In this context it is interesting to calculate the effective longitudinal (L_{eff}) and transverse (T_{eff}) force constants between the cation cores and the oxygen shells by summing the Coulomb and short-range contributions:

$$\begin{aligned} L_{eff} &= \tfrac{1}{2}([L_C + L_{sr}]_{long} + [L_C + L_{sr}]_{short}) \\ T_{eff} &= \tfrac{1}{2}([T_C + T_{sr}]_{long} + [T_C + T_{sr}]_{short}) \end{aligned} \tag{3}$$

The subscripts long and short in equation (3) indicate that we are averaging over the long and short bonds within a tetrahedron, respectively. The numerical values for these effective

Table 5. Intra-tetrahedral force constants for quartz and berlinite. L_C and T_C stand for the longitudinal and transverse force constants calculated from the Coulomb potential using the ionic charges listed in table 4. L_{sr} and T_{sr} denote the short-range force constants derived from the Born–Mayer potentials of table 4. The units are N m^{-1}. The numbering of the atoms refers to table 1 of this paper in the case of berlinite and to table 1 of Schober *et al* (1993) in the case of quartz.

Interaction	Bond length (Å)	Model	L_C	T_C	L_{sr}	T_{sr}
Si(1)–O(4)	1.6072	SM(1)	−889	445	1305	−170
Si(1)–O(6)	1.6100	SM(1)	−885	442	1239	−168
P(4)–O(13)	1.5122	SM(2)	−1334	667	1936	−268
P(4)–O(9)	1.5197	SM(2)	−1315	657	1867	−257
Al(1)–O(7)	1.7324	SM(2)	−532	266	719	−87
Al(1)–O(15)	1.7455	SM(2)	−521	260	675	−81

force constants are listed in table 6 for quartz (model SM(1)) and berlinite (model SM(2)). By comparing columns 2–4 of table 6 we realize that the bond strengths, as given by our lattice-dynamical models, differ strongly for Si–O, P–O and Al–O. If we average, however, the Al–O and P–O effective force constants they are nearly exactly as large as the ones for Si–O. The observation that the averaged effective force constants in berlinite are nearly identical to the effective force constants in quartz is in agreement with the results of earlier lattice-dynamical studies. Bethke *et al* (1992), with their simple short-range model, obtain close-lying values for the Al–O and P–O force constants on one hand and the Si–O force constants on the other hand. Given the resemblance of the dispersion curves such a similarity of the average cation–oxygen bond strength would be expected, especially in the light of the small mass differences of quartz and berlinite. It is, however, not a sufficient explanation for the fact that the strong differences in the Al–O and P–O force constants, as given by our models, do not show up in the optical frequencies.

As the interactions in our models are specified between oxygen shells and cation cores a direct comparison with equivalent interactions in rigid-ion models is generally excluded†. In the case of quartz we observe, however, that despite the rather large polarizability of the oxygen ion the longitudinal effective Si–O force constant of model SM(1) (385 N m^{-1}) differs only slightly from the values obtained for rigid-ion models ($\sim$ 400 N m^{-1}, see Barron *et al* (1976)). As the polarizability of the oxygen ion is unchanged, we may use this observation to perform a crude comparison of the shell models for berlinite with results obtained for other crystals containing PO_4 groups based on rigid-ion models. In this context, systems where the $(PO_4)^{3-}$ molecule is only weakly influenced by the crystal environment are of special interest. Using a rigid-ion approach the longitudinal P–O force constants for these crystals can be evaluated more or less directly from the measured frequencies of the molecular vibrations (see Herzberg 1945). One obtains values of approximately 600 N m^{-1} (Boyer and Fleury 1974) or 540 N m^{-1} (Herzberg 1945). These values are considerably higher than the value of the longitudinal P–O force constant (450 N m^{-1}) as given by Bethke *et al* (1992) for their rigid-ion model. But they are nearly identical to the value of the effective P–O force constant as given by model SM(2) (577 N m^{-1}). To exclude as much as possible the influence of the oxygen polarizability on our conclusions let us compare the ratio

† By inspection of table 6 we observe e.g. that for the shell models the strength of the transverse effective force constants of the cation–oxygen interaction is of the same order of magnitude as the one of the longitudinal effective force constants, while in the case of rigid-ion models (see Bethke *et al* 1992) the transverse force constants are about ten times weaker than the corresponding longitudinal force constants. As we will explain in section 6, these strong differences can be understood on the basis of the equilibrium conditions.

$$\frac{2L_{\text{eff}}(\text{P–O})}{L_{\text{eff}}(\text{P–O}) + L_{\text{eff}}(\text{Al–O})} \approx 1.5 \tag{3a}$$

obtained with the shell model force constants with the ratio

$$\frac{L_{\text{molecule}}(\text{P–O})}{L_{\text{berlinite}}(\text{P–O})} \approx 1.3 \tag{3b}$$

obtained with rigid-ion model force constants. If berlinite were a molecular crystal the ratio (3*a*) should be larger than unity, while (3*b*) should be equal to unity. In the case of an oxygen framework crystal just the opposite relations should hold. So, while the results of Bethke *et al* (1992) constitute strong evidence for the absence of $(PO_4)^{3-}$ units in berlinite—the binding of phosphorus to the oxygen ions is weaker than in the molecule, our models support the picture of a $(PO_4)^{3-}Al^{3+}$ crystal.

Table 6. Effective force constants as defined in equation (3) for model SM(1) (quartz) and SM(2) (berlinite). By average we denote the effective force constants in berlinite, which we obtain by averaging over the P–O and Al–O bonds. The units are N m^{-1}.

	Si–O	P–O	Al–O	Average ($AlPO_4$)
L_{eff}	385	577	171	374
T_{eff}	275	400	179	290

From the above discussion it becomes evident that special care must be taken when interpreting the results obtained by lattice-dynamical models, in particular if only a limited aspect of the vibrational spectrum is taken into consideration. Using different phenomenological models and concentrating on different parts of the vibrational spectrum two completely different pictures for the bonding in berlinite emerge. Whereas the results of Bethke *et al* (1992) suggest an oxygen framework structure our investigations lead to strongly bonded PO_4 units connected by aluminium ions. In the light of the dispersion relations alone both pictures are equally valid. By investigating the dielectrical properties as well as the equilibrium conditions in the following sections of this paper we will try to give further arguments in favour of our interpretation.

Before doing so, we present a second shell model for berlinite. By inspection of table 3 we find that the largest differences between the experimental data and the predictions of model SM(2) arise for the highest frequencies. A better agreement can be achieved if we take the ionic charges as free parameters. The values obtained for the ionic charges after adjustment of all model parameters to the experimental data are smaller than the valence charges of $-2e$ and $5e$ for the oxygen and phosphorus ions, respectively. As we will show in section 5 this lowering of the ionic charges with respect to quartz is also required by the observed LO–TO splitting. It turns out that the quality of the fit is hardly changed if we retain the same potential for the Al–O and P–O bonds. In contrast to model SM(2), however, both the amplitude V_0 and the decay constant a (see equation (1)) differ from the parameters obtained for quartz. In addition, there is no need for a short-range potential between oxygen cores if we specify Keating potentials within the PO_4 tetrahedra as well as for the inter-tetrahedral angles. Together with the ionic charges the thus-constructed model, which we call SM(3), has the same number of free parameters as model SM(2). However, all 10 parameters of model SM(3) are adjusted to the experimental frequencies of berlinite and not taken over from a similar model for quartz. The final parameter values after the adjustment are shown in table 4 and the calculated Γ-point frequencies in table 3. Although the agreement with the experimental data could be improved slightly with respect to model

SM(2), the outstanding quality of model SM(3) resides in the fact that the dynamics of berlinite is described in terms of valence forces, while a direct oxygen–oxygen potential is included in model SM(2). It is, therefore, easier to discuss the bonding in berlinite on the basis of model SM(3) instead of model SM(2).

The intra-tetrahedral valence forces are only significant for the PO_4 groups while for the AlO_4 groups an inclusion of this type of interaction does not result in a better model. This observation is consistent with the x-ray results of Schwarzenbach (1966) which show that the P–O bond is more covalent than the Al–O bond. An important point in connection with Keating potentials is the value of the parameter β' (see equation (2)). In a crystal described by Keating potentials only, equilibrium can be ensured by requiring that β' is identical to one for all interactions. This is a consequence of the rotational invariance of the potential. If we interpret the parameter β' in such a sense that the angle for which the potential is in equilibrium may differ slightly from the angle found for the actual crystal structure then values for β' very much different from one are not permitted. The values of 1.3 and 1.5 for the inter- and intra-tetrahedral Keating parameters β', respectively, are, therefore, a positive indication for the physical correctness of the potentials.

As already mentioned above, no model equivalent to SM(3) has been investigated for quartz. In order to answer the question of whether the direct oxygen–oxygen interactions present in the quartz models are indispensable for the description of its lattice dynamics we applied model SM(3) to the quartz structure. Without any adjustment of the parameters model SM(3) reproduces the dispersion curves of quartz rather poorly. As our main interest in applying model SM(3) to quartz concerns the changes in bonding we did refrain from adjusting all parameters of the model. Indeed it turns out that a very satisfactory description of the experimental data can already be achieved by fitting the Keating parameters only. The values obtained for this quartz model, which will be denoted SM(4), are given in table 4. The calculated dispersion curves for the Γ–A direction, together with the experimental data of Strauch and Dorner (1993), are shown in figure 2.

Although there are some discrepancies for the higher branches the overall description of the dispersion curves is good and the same can be said for the Γ–M direction.

The changes of the Keating parameters taking place when going from berlinite to quartz are particularly strong for the inter-tetrahedral angles (see table 4). This indicates that the mechanism responsible for the connection of the SiO_4 tetrahedra in quartz via the oxygen ions differs both in character—$\beta'_{\text{inter}}(AlPO_4) = 1.3$; $\beta'_{\text{inter}}(SiO_2) = 4.2$—and in strength—$\beta_{\text{inter}}(AlPO_4) = 16.8$ N m^{-1}; $\beta_{\text{inter}}(SiO_2) = 1.6$ N m^{-1}—from the mechanism connecting PO_4 to AlO_4 tetrahedra in berlinite. This interpretation is consistent with the observation that the quality of model SM(4) can be improved by including a direct silicon–silicon interaction (the numerical values are given in parenthesis in table 4). An equivalent interaction between aluminium and phosphorus ions in model SM(3) for berlinite proved, in contrast, inefficient. As can be seen in table 4, a direct silicon–silicon interaction implies considerable changes in the Keating parameters for the inter-tetrahedral angles—$\beta_{\text{inter}}(SiO_2) = 5.1$ N m^{-1}; $\beta'_{\text{inter}}(SiO_2) = 2.5$, to be compared with the above-mentioned values—hinting at a strong correlation of the two interactions. It should be pointed out that the inter-tetrahedral Keating potentials for model SM(4) with direct silicon–silicon interactions are closer to the ones of model SM(3). In particular, the value of the β' parameter is more physical. In conclusion, it seems that while the inter-tetrahedral bonding in berlinite can be well described by Keating potentials, this is only partly true in the case of quartz.

Compared to the inter-tetrahedral interactions the intra-tetrahedral interactions change mainly in strength when going from berlinite to quartz—$\beta_{\text{intra}}(AlPO_4) = 6.7$ N m^{-1}; $\beta_{\text{intra}}(SiO_2) = 3.3$ N m^{-1}—and less in character—$\beta'_{\text{intra}}(AlPO_4) = 1.5$; $\beta'_{\text{intra}}(SiO_2) = 2.0$.

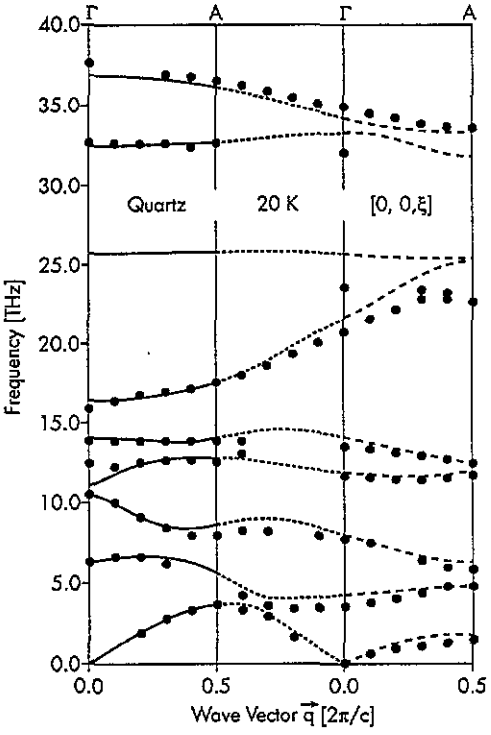

Figure 2. Dispersion curves of α-quartz at 20 K for the Γ–A direction. Symbols: experimental frequencies (Strauch and Dorner 1993); lines: theoretical results from shell model SM(4). An extended-zone scheme is used to plot the dispersion curves for the three different irreducible representations separately.

Although this result has to be interpreted with care, as we cannot be sure that the Keating potentials describe the covalent bonding in tetrahedrally coordinated oxides perfectly, it clearly indicates the strong covalent character of the O–P–O bond.

5. Charges and polarizabilities

As has been discussed extensively by Schober and Strauch (1993) the study of the LO–TO splitting is a practical tool to predict charges and polarizabilities in crystals like quartz. The central quantity of interest in this context is Ω^2, as defined through equation (4), which is a measure of the optical splitting.

$$\Omega^2 = \sum_{i=1}^{3(n_r-1)} (\omega_i^{LO}(q)^2 - \omega_i^{TO}(q)^2) \qquad |q| \to 0 \tag{4}$$

where ω^{LO} and ω^{TO} denote the longitudinal and transverse frequencies, respectively. The values of Ω^2 for quartz and berlinite, as calculated by using the experimental frequencies, are given in table 7.

As can be seen, the value of Ω depends on the set of experimental data used for its calculation. Comparing the values of Ω obtained using the experimental frequencies of Camassel *et al* (1988) we observe no variations with the respective phonon representations, i.e. the direction of q. This is to be expected given the values for quartz and the small anisotropy of the high-frequency dielectric tensor in berlinite (see table 8). We will come back to the latter point further on in the discussion. The observed isotropy of Ω as a function of q, therefore, speaks in favour of the data of Camassel *et al*. A similar test for the Raman

Table 7. Values of $\nu_\Omega = \Omega/2\pi$ as defined by equation (4) in units of THz. The experimental values were obtained with the frequencies given by Camassel *et al* (1988) and by Scott (1971) (marked by an asterisk) for berlinite and of Elcombe (1967) for quartz. In column one we give the respective phonon representations.

	α-quartz		α-berlinite			
Representation	Experiment	SM(1)	Experiment		SM(2)	SM(3)
$\nu_\Omega(\Gamma_2)$	20.4	19.7	—	19.2	21.7	17.5
$\nu_\Omega(\Gamma_3)$	20.4	19.7	20.5*	19.3	21.2	17.4
$\nu_\Omega(\frac{1}{3}(\Gamma_2 + 2\Gamma_3))$	20.4	19.7	—	19.3	21.5	17.5

Table 8. High-frequency dielectric constants. Experimental values taken from Gervais and Piriou (1975) (infrared spectroscopy) and Bond (1965) (reflectivity measurements: $\lambda = 1.6\ \mu$m) for quartz and berlinite, respectively. ϵ^∞_{xx} and ϵ^∞_{zz} are the two independent elements of the dielectric tensor.

	α-quartz		α-berlinite		
	Experiment	SM(1)	Experiment	SM(2)	SM(3)
ϵ^∞_{xx}	2.36	2.36	2.28	2.38	2.28
ϵ^∞_{zz}	2.38	2.37	2.30	2.41	2.30

frequencies of Scott is not possible as the modes of the Γ_2 representation are not Raman active.

Before comparing the calculated with the experimental values we want to express Ω in terms of effective charges and the high-frequency dielectric constants.

Let us define the effective charge tensor in the usual way through

$$\omega^2 \mathbf{M}\mathbf{u} = \mathbf{D}^{\text{reg}}\mathbf{u} - e(\mathbf{Z}^{\text{eff}})^{+}\mathbf{E}^{\text{mac}} \tag{5}$$

where $\mathbf{D}^{\text{reg}}$ is a regular matrix for $|q| \to 0$ and $\mathbf{E}^{\text{mac}}$ is the macroscopic electromagnetic field associated with the respective lattice vibration. $\mathbf{M}$ is the mass tensor.

It has been shown (see Schober and Strauch (1993)) that for a general system with diagonal dielectric tensor Ω can be expressed as

$$\Omega^2 = \frac{4\pi e^2}{3v}\,\mathrm{Tr}(\epsilon^\infty(\hat{q})^{-1}) \sum_\kappa \frac{1}{M(\kappa)} \sum_{\sigma\alpha} (Z^{\text{eff}}_{\sigma\alpha}(\kappa))^2 \tag{6}$$

with

$$\epsilon^\infty(\hat{q}) := \hat{q} \cdot \epsilon^\infty \cdot \hat{q} \tag{6a}$$

$$Z^{\text{eff}}_{\alpha\beta}(\kappa) := \sum_{\kappa'} Z^{\text{eff}}_{\alpha\beta}(\kappa', \kappa). \tag{6b}$$

κ and κ' designate the ions in the primitive cell and v is the cell volume. In order to avoid confusion with the notation we want to stress that while the effective charge tensor $\mathbf{Z}^{\text{eff}}$ is a $(3r \times 3r)$ matrix $\mathbf{Z}^{\text{eff}}(\kappa)$ denotes a (3×3) matrix specific to the ion of type κ.

In the case of rigid-ion models the effective charge tensor is necessarily diagonal and we may replace $\sum_{\alpha\sigma}(Z^{\text{eff}}_{\sigma\alpha}(\kappa))^2$ by $3(Z^{\text{eff}}(\kappa))^2$, where $Z^{\text{eff}}(\kappa)$ is an arbitrary diagonal element of the (3×3) tensor $Z^{\text{eff}}_{\alpha,\sigma}(\kappa)$. By defining, in analogy,

$$Z^{\text{eff}}(\kappa) := \frac{1}{\sqrt{3}}\,\mathrm{sign}(Z_\kappa)\sqrt{\sum_{\alpha\sigma}(Z^{\text{eff}}_{\sigma\alpha}(\kappa))^2} \tag{7}$$

we write equation (6) in the form

$$\Omega^2 = \frac{4\pi e^2}{v} \mathrm{Tr}(\epsilon^{\infty}(\hat{q})^{-1}) \sum_{\kappa} \frac{(Z^{\mathrm{eff}}(\kappa))^2}{M(\kappa)} \tag{8}$$

for an arbitrary crystal. Please note that the sign of the scalar effective charges $Z^{\mathrm{eff}}(\kappa)$ as defined through equation (7) is given by the sign of the ionic charges. In general the scalar effective charges do not fulfil a sum rule, although the corresponding charge tensors $\mathbf{Z}^{\mathrm{eff}}(\kappa)$ do:

$$\sum_{\kappa} Z^{\mathrm{eff}}_{\alpha\beta}(\kappa) = 0. \tag{9}$$

Only in the case of rigid-ion models, for which the effective charges $Z^{\mathrm{eff}}(\kappa)$ are identical to the ionic charges Z_{κ}, do they add up to zero as a consequence of the charge neutrality of the crystal. The violation of the sum rule for $Z^{\mathrm{eff}}(\kappa)$, i.e. the non-zero value of

$$\Delta(Z^{\mathrm{eff}}) := \sum_{\kappa} Z^{\mathrm{eff}}(\kappa) \tag{10}$$

is due to the off-diagonal elements of $\mathbf{Z}^{\mathrm{eff}}(\kappa)$.

Table 9. Effective charges as defined by equations (7) and (10) in units of e.

	α-quartz	α-berlinite	
	Model SM(1)	Model SM(2)	Model SM(3)
$Z^{\mathrm{eff}}_{\mathrm{O}}$	−1.82	−2.06	−1.63
$Z^{\mathrm{eff}}_{\mathrm{Si}}$	3.25	—	—
$Z^{\mathrm{eff}}_{\mathrm{Al}}$	—	3.05	1.89
$Z^{\mathrm{eff}}_{\mathrm{P}}$	—	4.01	3.52
$\Delta(Z^{\mathrm{eff}})$	−0.39	−1.18	−1.11

Besides the effective charges it is the high-frequency constant ϵ^{∞} which determines the optical splitting (see equation (10)). Schober and Strauch (1993) argued that ϵ^{∞} should scale linearly with the effective polarizability

$$\epsilon^{\infty} = 1 + \frac{4\pi}{v} r_{\mathrm{p}} \alpha_{\mathrm{eff}} \tag{11}$$

which has been defined as follows:

$$\alpha_{\mathrm{eff}} := (\alpha^{-1} + \phi)^{-1} \tag{12}$$

where α is the polarizability of the hypothetical free ion and ϕ is a function of the self-terms of the polarizable ions (see Schober and Strauch 1993). Although equation (11) has been deduced rigorously only for binary crystals, it can safely be applied to berlinite, as like quartz berlinite features only one type of polarizable ion†. As ϕ is a function of the self-terms it is only sensitive to *average* changes in the force constants, acting upon the

† We assume that the two types of oxygen ion present in berlinite are, from a chemical point of view, identical, in particular, that they have the same charges and polarizabilities.

polarizable ions. In section 4 we have found that these average changes are very small when going from quartz to berlinite. Therefore, α_{eff}, and in consequence ϵ^{∞}, should be very similar for both substances. This is actually confirmed both by experiment and by our numerical calculations. While the theoretical values for ϵ^{∞} are somewhat too large for model SM(2) the agreement is excellent for model SM(3) (see table 8). Both the theoretical and the experimental values show that the dielectric tensor is nearly isotropic. This is a necessary condition for the validity of equation (11).

The investigation of the dielectric constants, therefore, indicates that the polarizability of the hypothetically free oxygen ion should be about 1.8 Å^3 as in quartz†. We can interpret this similarity of the polarizabilities microscopically by expressing α_{eff} in terms of matrix elements between occupied orbitals ϕ_i and unoccupied orbitals ϕ_j (see Pantelides 1975, Pantelides and Harrison 1976)

$$\alpha_{\text{eff}} = 2e^2 \sum_{i,j} \frac{|\langle\phi_i|x|\phi_j\rangle|^2}{E_j - E_i}. \tag{13}$$

E_i and E_j are the respective energies of the orbitals. If the electronic distribution around the oxygen ion is similar in quartz and berlinite both for the conduction and valence bands then α_{eff} is not expected to change strongly as the main transitions between valence and conduction bands are localized at the oxygen ion (see Binggeli *et al* 1991, Chelikowski *et al* 1990). Turning the argument around, we may take the nearly identical values of α_{eff} in quartz and berlinite as an indication for similar charge states of the oxygen ion.

As already mentioned above, no sum rule holds for the effective charges. Therefore, we cannot determine the effective charges directly from the experimental values of Ω and ϵ^{∞} using equation (8). In the case of binary crystals like quartz the problem can be circumvented by expressing Ω analytically as a function of the ionic instead of the effective charges (see Schober and Strauch 1993). This procedure does not, however, work for ternary compounds like berlinite due to the possibility of distributing the positive charges unequally among the cations. We, therefore, can only place upper and lower limits, albeit rather precise, on the charges. Let us start with an oxygen charge of $-2e$. This fixes at the same time all the other charges and we are left with model SM(2). Model SM(2) overestimates the splitting of the optical modes. The ionic charge of the oxygen must therefore be smaller than $-2e$, which also means smaller than the value we have deduced for α-quartz. Model SM(3) with an oxygen charge of $-1.68e$ underestimates the splitting. Although we cannot exclude the possibility that the LO–TO splitting might be increased by appropriately changing the cation charges only, thus allowing for a still smaller oxygen charge, such a further reduction of Z_{O} would imply a simultaneous decrease of the polarizability α. The latter is excluded on the basis of ϵ^{∞}. Our considerations, therefore, converge towards a shell model with an ionic oxygen charge around $-1.8e$. As Z_{Al} can hardly exceed $3e$ charge neutrality together with $Z_{\text{O}} = -1.8e$ implies $Z_{\text{P}} \geqslant 4.2e$, i.e. a rather unequal distribution of the positive charges among the cations.

In contrast to what was thought earlier (Scott 1971), this picture of a strongly ionic crystal is, as our calculations show, perfectly compatible with the experimental data. Based on the assumption that the effective charge of the oxygen ion in berlinite does not differ strongly from the one in quartz Scott concluded from the optical splitting through equations (8) and (9) that the difference in the effective charges of aluminium and

† To reach this conclusion through equation (11) we must assume that the value of ϕ is only weakly model dependent, as this is the case for quartz.

phosphorus must be rather small ($Z_P^{eff} - Z_{Al}^{eff} \leqslant 0.2\epsilon^{\infty}e \simeq 0.45e$). Although the assumption of a similar effective charge for the oxygen ion in quartz and berlinite is confirmed by our calculations (see table 9) the proposed limit for $Z_P^{eff} - Z_{Al}^{eff}$ is at variance with our results. The reason for the failure of Scott's simple approach is, to our opinion, rooted in the contributions of the short-range interactions to the effective charges†. Due to the anisotropy of the charge tensor $\mathbf{Z}^{eff}$ the sum rule (equation (9)) is not applicable to the scalar effective charges defined through equation (7), thus invalidating one essential step in Scott's arguments. To demonstrate the violation of the sum rule we have included the quantity $\Delta(Z^{eff})$, as defined through equation (10), in table 9.

6. Equilibrium conditions

As all the models for berlinite are based on potentials (Coulomb, Born–Mayer, Keating) only, the forces acting upon the ions can be calculated directly using the first derivatives of these potentials. As in the case of quartz (Schober *et al* 1993) it turns out to be impossible to satisfy simultaneously all 10 equilibrium conditions, corresponding to the 10 structural parameters in berlinite, with the limited number of parameters we use to describe the dynamics. The deviations become the more important the higher the charges.

As the oxygen ion is highly polarizable in all our models, the non-vanishing electrostatic field at the oxygen sites must inevitably lead to static dipole moments, which have to be included in the equilibrium conditions. In principle the static dipoles can be simulated in the framework of shell models by placing the shells off-centre from the cores (see e.g. Dove 1989). As the short-range forces mainly act upon the shells, the inclusion of static dipoles through off-centre positions for the shell changes the short-range part of the equilibrium conditions themselves, thus requiring a self-consistent calculation. The large number of extra parameters introduced into the models (six for the two types of oxygen in berlinite) together with the uncertainties in the short-range potentials themselves do not, in our opinion, warrant such a rather involved procedure.

Instead, we follow a different route. The fact that both AlO_4 and PO_4 tetrahedra can be found in a large number of crystals suggests that these tetrahedra are more or less stable in themselves independent of the crystalline environment. If this is the case we may build up an idealized $AlPO_4$ structure by assembling regular PO_4^{Z-} tetrahedra and Al^{Z+} ions, or, alternatively, AlO_4^{Z-} tetrahedra and P^{Z+} ions. For non-zero charges Z such a crystal is not in equilibrium due to the electrostatic forces acting among the building blocks. Equilibrium can, however, be achieved in two ways: first by allowing for appropriate relaxation through distortions of the tetrahedra‡ and second by compensating electrostatic forces through static dipole moments.

In order to check the validity of such an approach we must first investigate the underlying assumption, i.e. the equilibrium of the isolated tetrahedra. Taking into consideration the interactions of the shell models described in section 4 and assuming that the shells are clamped at the core positions, equilibrium for these isolated tetrahedra is achieved if

$$A - (B + C) = 0$$

† By inspection of table 9, we observe that the influence of the short-range forces on the effective charges is rather limited in the case of the oxygen ion, in particular for the models of berlinite. The same statement holds for the aluminium ions. Large differences with respect to the ionic charges occur, however, for the phosphorus and silicon ions.

‡ Such distortions also have to meet geometrical constraints. Regular tetrahedra are incompatible with the quartz structure unless they are of specific size. This size is a function of the two lattice constants a and c (see Smith 1963).

with

$$A = \frac{1}{r}\left[\frac{V_{(K-O)}}{a_{(K-O)}}\exp\left(-\frac{r}{a_{(K-O)}}\right) + \frac{\eta}{\zeta}\frac{V_{(O-O)}}{a_{(O-O)}}\exp\left(-\frac{\zeta r}{a_{(O-O)}}\right)\right]$$
$$B = -\eta\frac{18\sqrt{3}-5}{7\sqrt{3}-3}\beta(1-\beta') \qquad C = -\frac{e^2}{4\pi r^3}\left[Z_O Z_K + \frac{\eta}{\zeta^3}Z_O^2\right]. \tag{14}$$

A is the contribution from the cation–oxygen (subscript: K–O) and oxygen–oxygen (subscript: O–O) Born–Mayer potentials (equation (1)), B the contribution from the intra-tetrahedral Keating potentials (equation (2)) and C the Coulomb part. Please note that, in general, the charge of the cation Z_K is not fixed by the oxygen charge Z_O in structures consisting, like berlinite, of several non-equivalent tetrahedra. Equation (14) contains only one length scale given by the cation–anion nearest-neighbour distance r. This is due to the fact that it was set up for regular tetrahedra, only. Equation (14) may therefore be applied to any member of the quartz-family but also to zeolite and any other substance containing AO_4 tetrahedra.

There are two geometrical factors η and ζ entering equation (14). The factor ζ is given by the ratio of the cation–anion over the anion–anion distance which, for a regular tetrahedron, is equal to $\zeta = 4/\sqrt{6}$. The factor η arises from the projection of the forces acting upon the anions onto the cation–anion direction and, for a regular tetrahedron, is identical to four. Normally, at least for small distortions, these values for η and ζ can also be applied to distorted tetrahedra. This holds in particular if, as in the case of quartz and berlinite, the tetrahedra possess a twofold axis of symmetry.

Given a specific lattice-dynamical model we may use equation (14) to determine the cation–anion distances for which the tetrahedra of the crystal are in equilibrium. For the quartz models SM(1) and SM(4) we find r(Si–O) = 1.59 Å and 1.61 Å, respectively. This is in excellent agreement with the experimental value of 1.61 Å for the average silicon–oxygen distance (see table 2), in particular as we necessarily introduce a slight error into the calculation by considering clamped shells, only. In silicate minerals the oxygen shell position deviates from the core position by typically 0.01 – 0.02 Å for non-clamped shells (see Dove 1989). The equilibrium distances for the berlinite model SM(2) are r(P–O) = 1.51 Å and r(Al–O) = 1.73 Å, while for model SM(3) we find r(P–O) = 1.46 Å and r(Al–O) = 1.77 Å. These values have to be compared with the experimental values of r(P–O) = 1.52 Å and r(Al–O) = 1.74 Å. For model SM(2) we observe as in the case of quartz very good agreement between theory and experiment. Only in the case of model SM(3) are larger discrepancies observed for the P–O distances. In our opinion the difficulty of model SM(3) to predict the equilibrium P–O distance correctly through equation (14) has its origin in the fact that we force the model to describe both the P–O and the Al–O interactions by identical short-range potentials. The fulfilment of equation (14) by the potentials of model SM(3) for quartz tetrahedra is, on the other hand, a good precondition for the transferability of these potentials from one substance to the other.

The contributions of the Keating potentials are very important for the correct prediction of equilibrium distances through equation (14). Without these contributions the errors would be larger by as much as 0.05 Å. This is only possible as the Keating parameter β' deviates from its ideal value of unity. As outlined in the previous section, Keating potentials in their pure form, i.e with $\beta' = 1$, do not contribute to the equilibrium conditions as they are rotationally invariant (see Boyer 1974, Keating 1966).

Condition (14) places severe constraints on the model potentials. Given the Coulomb charges both parameters of the short-range Born–Mayer potential are determined in a simple

model like SM(3). As the fulfilment of the equilibrium condition has at no stage been part of the fitting process, the fact that this condition is so well satisfied by our models constitutes a strong argument in favour of the physical reality of the potentials used.

We may summarize this section as follows. The interionic potentials which have been designed to describe the dynamics of quartz and berlinite automatically predict the correct size for the constituent tetrahedral units through equation (14). This result justifies the picture of crystals which can be thought of as being built up from isolated molecules. The additional forces arising from assembling the charged units are absorbed by an appropriate relaxation of the crystal structure. In principle, the relaxation is a complex process in the course of which the interionic potentials themselves readjust. It is, therefore, by no means evident that the potentials in the crystal should be the same as the ones within isolated tetrahedra. In particular, they may predict equilibrium bond lengths for these tetrahedra different from the ones in the crystal. However, due to the strength of the intra-tetrahedral bonding in these crystals even displacements of the ions which are small compared to the range of the potentials are sufficient to compensate large static forces. It is, therefore, to be expected that the influence of the relaxation process on the potentials is limited explaining the good fulfillment of equation (14). The situation changes if the compensation of the static forces can only be achieved through a reorientation of the tetrahedra with respect to each other. In this case large atomic movements are possible which dynamically may find their expression in soft-going modes and finally in a phase transition.

If the potentials we have found are the actual physical potentials and if the above picture is correct then these potentials should in principle also predict equilibrium for the crystal after relaxation. This is, however, as mentioned at the beginning of this section, not the case. Although the size of the tetrahedra comes out right, the overall crystal structure, which is mainly determined by the inter-tetrahedral angles, is not predictable by our model. One explanation for this failure is certainly to be found in the necessary appearance of static dipole moments. On the other hand we surely do not describe every detail of the interionic bonding by our simplified models. In particular, the forces arising from the low-lying electronic bands and responsible for the strong covalent bonding but with limited influence on the dynamics are probably ill described by our potentials.

7. Temperature dependences

As outlined in section 2 both quartz and berlinite show a phase transition to a higher-symmetry modification. With $T_0 \approx 846$ K for SiO_2 and $T_0 \approx 857$ K for $AlPO_4$, these transitions take place at nearly the same temperature. One should, therefore, expect a common mechanism to be responsible for these transitions. Given the similarities in the crystal structures, the fact that the dynamics can be described by common potentials supports this point of view.

If we interpret our model potentials as the real interatomic potentials then we can in principle calculate anharmonic corrections by using a mean-field theory. These mean-field calculations must imperatively be done self-consistently. A non-self-consistent calculation leads to the well known result that near the critical temperature the squared frequency of the soft mode is a linear function of $T - T_0$ and that the slope of this function for $T < T_0$ is -2 times the slope for $T > T_0$. A comparison of the soft-mode frequencies above and below the phase transition reveals that this requirement is incompatible with the

experimental findings†. Self-consistent mean-field theory for a complicated structure like quartz is very tedious and its success is by no means guaranteed. As we will show in the following discussion, there are several indications that a mean-field treatment, even when done self-consistently, may be unable to explain the transition mechanism.

In table 10 we have listed the cation–anion distances in quartz and berlinite as a function of temperature. For both structures the respective tetrahedra contract when going from the α- to the β-modification, while the unit cell expands. This contraction of the tetrahedra implies that, if we transfer the potentials found at room temperature for the α-modifications unchanged to the β-modifications, the force constants derived from the potentials will increase. This is at variance with the usual softening of the force constants with rising temperature. Due to the rather small cut-off a of the Born–Mayer potentials this increase in force constants and the corresponding overall increase of the frequencies is rather strong. For certain frequencies it may attain 10%. Such changes in frequency are not observed experimentally. On the contrary, apart from the soft-going modes the overall spectrum shows hardly any temperature dependence at all (see Gervais and Piriou 1975). The increase in force constants must, therefore, be compensated. This compensation may either be due to anharmonic terms or to changes in the potential itself, i.e. violations of the adiabatic condition. Anharmonic terms based upon the Born–Mayer potential at room temperature will hardly give the desired result, as they would also lead to an expansion of the tetrahedra with increasing temperature.

Table 10. Temperature dependence of the cation–anion distances in quartz and berlinite according to Grimm and Dorner (1975) and Ng and Calvo (1976), respectively. For experimental errors see the original papers. The numbering of the ions refers to table 1. The subscript av denotes average bond distances for the respective terahedra. The bond distances for β-quartz have been calculated for two different values of the structural parameter y according to Young (1962) and Wright and Lehmann (1981) at $T = 863$ K.

	α-quartz						β-quartz	
T (K)	300	573	723	800	823	840	$y = 0.207$	$y = 0.211$
r(Si(1)–O(6)) (Å)	1.608	1.601	1.594	1.582	1.583	1.578	1.594	1.582
r(Si(1)–O(4)) (Å)	1.610	1.607	1.600	1.600	1.606	1.607	1.600	1.600
r_{av}(Si–O) (Å)	1.609	1.604	1.597	1.591	1.594	1.593	1.597	1.591
	α-berlinite						β-berlinite	
T (K)	300	723	773	800	823	853	873	
r(Al(1)–O(7)) (Å)	1.73	1.73	1.66	1.68	1.68	1.73	1.69	
r(Al(1)–O(15)) (Å)	1.74	1.74	1.68	1.70	1.61	1.62	1.69	
r_{av}(Al–O) (Å)	1.73	1.74	1.67	1.69	1.65	1.67	1.69	
r(P(4)–O(13)) (Å)	1.53	1.51	1.56	1.54	1.59	1.58	1.51	
r(P(4)–O(9)) (Å)	1.52	1.51	1.55	1.49	1.48	1.43	1.51	
r_{av}(P–O) (Å)	1.52	1.51	1.56	1.52	1.53	1.51	1.51	
r_{av}(P–O + Al–O) (Å)	1.63	1.62	1.615	1.605	1.59	1.59	1.60	

As we have seen in the preceding section the equilibrium of the tetrahedra plays a central role in all our models. Due to the contraction of the tetrahedra the equilibrium condition

† We will not go into the discussion of the incommensurable phase observed in the small temperature range between the low- and high-symmetry modifications (see Bethke *et al* 1987), as this problem can hardly be treated by our simplified approach.

(14) cannot be satisfied by one single set of potential parameters for different temperatures. By requiring the fulfilment of equation (14) for all temperatures we obtain a one-to-one correspondence of a chosen model parameter, in our case the cut-off constant a of the cation–anion potential, with temperature. The rest of the parameters are kept constant. We choose to adjust the short-range potential‡ and not the charges as neither the splitting of the polar modes nor the high-frequency dielectric constants show any temperature dependence (see Gervais and Piriou 1975). A change of the charges with temperature is, therefore, practically excluded. The same holds for the polarizability α which anyway does not enter the equilibrium condition (14)§. In figure 3 we show the parameter a as a function of temperature for the quartz model SM(1).

There is some arbitrariness the procedure outlined stemming from the fact that the temperature dependence of the short silicon–oxygen bond differs from the one for the long silicon–oxygen bond. Upon inspection of table 10 we find that only the short bond is appropriate for our purpose as it shows a monotonic behaviour with temperature. Instead of defining $a(T)$ through equation (14) we may also use the experimentally established invariance of certain phonon frequencies for its definition. The situation does not improve noticably due to the arbitrariness in choosing the frequencies. It is, however, reassuring, that both procedures give nearly identical results, the reason being that they both amount to keeping the force constants more or less unchanged with temperature.

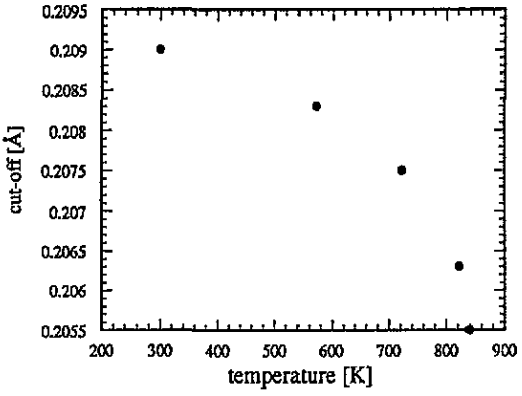

Figure 3. Cut-off parameter a of the cation–anion potential of model SM(1) as a function of temperature.

Having established the temperature dependence of the model parameters we can calculate the frequency spectra on the basis of the experimentally determined structural changes. It turns out that most of the modes show only a very weak temperature dependence, exactly as required by experiment. Exceptions to this rule are the soft modes at the Γ and M points, the frequencies of which approach zero at the phase transition. In the case of the M-point modes the temperature dependence of the frequencies as given by our model is confirmed by experiment (Boysen *et al* 1980). For the Γ-point mode the experimental situation is less clear as one- and two-phonon Raman excitations mix at higher temperatures (see the discussion by Scott (1968) and the paper by Shapiro *et al* (1967). Above T_0 a small change in the transverse oxygen–oxygen force constants ($\sim$ 1 N m^{-1}) is necessary to reestablish stability, i.e. to regain a positive frequency spectrum for all modes. Within

‡ If the changes necessary are small, it does not matter whether we change the cut-off a or the amplitude V of the Born–Mayer potential.

§ Reminder: when deriving equation (14) we have considered the oxygen ions as clamped.

the β-phase the stability range of our models is very small†. Even small changes in the force constants lead to negative frequencies. As through the dependence of the potentials upon bond distances such changes can also be generated indirectly by variations of the structural parameters, the choice of these parameters strongly influences the predictions of the model calculations in the β-phase. Thus the experimental data (Bethke *et al* 1987) are reproduced better by model SM(1) if we use e.g. $y = 0.211$ as proposed by Young (1962) instead of $y = 0.207$ as proposed by Wright and Lehmann (1981)‡. Experimentally the limited stability range of the β-phase finds its expression in the fact that the soft mode stays at very low frequencies even at temperatures far above T_0.

Our results are very similar to the ones obtained by Barron *et al* (1976) for simple short-range models. To the extent that the polarizability of the oxygen ion plays a minor role in the mechanism of the phase transition these similarities can be understood on the basis of the small variations of the force constants imposed by the temperature dependence of the potentials.

Upon inspection of table 10 we find that it is very difficult to establish a temperature dependence $a(T)$ for berlinite by the procedures used for quartz. While in the case of quartz the average silicon–oxygen distance smoothly decreases with temperature the aluminium–oxygen and phosphorus–oxygen distances in berlinite vary in an irregular way. For the PO_4 tetrahedra we observe e.g. that the average cation–anion distance r rises from 1.51 Å to 1.56 Å between 723 K and 773 K followed by a sharp drop to 1.52 Å at 800 K. For comparison, in quartz the average silicon–oxygen distance decreases by just 0.02 Å between room temperature and T_0. Theses variations are even more pronounced if we look at the difference between the long and short P–O bonds§ within the tetrahedra. While these bond lengths are nearly equal at 773 K they differ by 0.05 Å at 800 K. Please note that these temperatures are not close to T_0. Such strong variations of bond lengths ($\sim$ 4%) over such a small temperature interval in the absence of a phase transition must be considered enormous. Anharmonic contributions to the potentials are in our opinion insufficient to explain the phenomenon. Therefore, if these variations are real, they have to be explained on the basis of changes in the electronic distribution, i.e. they are genuinely non-adiabatic in character. As these variations find their expression in the force constants derived from potentials, the compensation of the changes occurring with temperature—as required by the invariance of most frequencies and also by equation (14)—implies a strongly fluctuating function $a(T)$. We have no physical interpretation for such fluctuations and consider that the variations of bond lengths in α-berlinite have not received the necessary attention, either experimentally or theoretically.

As we have difficulties dealing with the irregular contractions of the tetrahedra within the α-phase, let us compare the room-temperature data with the ones for the β-phase only. This has the additional advantage that in these two cases the experimental errors for the bond lengths are small†. Consulting table 10, we find that for the AlO_4 tetrahedron the

† By stability range we denote the volume defined by the maximum allowed deviations of the model parameters (from their nominal values) which are still compatible with a positive vibrational spectrum. In general, the stability range of a model is given by a complicated volume in a p-dimensional space, where p is the number of free parameters. If one considers one parameter, only, this volume becomes a one-dimensional interval.

‡ It is interesting to note that while for $y = 0.211$ the two inequivalent oxygen–oxygen distances are nearly identical they differ strongly for $y = 0.207$. The same statement holds for the cation–anion distances as can be seen by inspection of table 10.

§ At $T = 853$ K the long P–O bond measures 1.58 Å, identical to the Si–O bond in quartz at that temperature, while the short P–O bond measures 1.43 Å.

† It has to be pointed out that the experimental errors for the bond lengths in berlinite are generally far larger than in quartz. Smaller errors would surely be desirable.

contraction ($\sim$ 0.03 Å) is somewhat larger than for the PO_4 tetrahedron ($\sim$ 0.01 Å). In terms of equation (14) both contractions are compatible with a single change of the Born–Mayer parameter a from 0.2035 Å at room temperature to 0.2005 Å in the β-phase and no changes otherwise. In addition, by making the same change to the potential of model SM(4), we achieve equilibrium also for the SiO_4 tetrahedra in quartz. This result simply reflects the fact that the contraction of the SiO_4 tetrahedra is intermediate to the contraction of the AlO_4 and PO_4 tetrahedra.

8. Conclusion

We have shown that, by making small changes to the shell models developed for α-quartz (SiO_2), it is possible to give a satisfactory description of the experimentally determined frequencies of berlinite ($AlPO_4$). In particular, the potential between silicon and oxygen ions in quartz can be used practically unchanged for the short-range interactions between aluminium and oxygen and phosphorus and oxygen ions in berlinite. This transferability is a strong indication that the cation-oxygen potentials in these materials are mainly determined by the oxygen ion.

Contrary to previous investigations (Bethke *et al* 1992, Scott 1971), all our models indicate that berlinite like quartz is a strongly ionic crystal with the positive charge unequally distributed among aluminium and phosphorus ions. Based on both the investigation of the high-frequency dielectric constant and the splitting of the polar modes we give rather precise estimates of the charges and polarizabilities in berlinite, independent of particular lattice-dynamical models. The charge of the oxygen ion should be close to $1.8 \pm 0.1e$ with the polarizability of the free ion lying between 1.7 and 1.9 Å^3. The ionic charges of the phosphorus and aluminium ions come out to be $4.5e$ and $2.25e$, respectively. Owing to the contributions from the short-range potentials the effective charges of the phosphorus and aluminium ions differ by smaller amounts than the respective ionic charges.

In what concerns the short-range interactions, the ones within the PO_4 tetrahedra clearly dominate in strength the ones within the AlO_4 tetrahedra. As, in addition, there is an appreciable covalent contribution to the bonding within the PO_4 tetrahedra, while no signs for such bonding can be detected within the AlO_4 tetrahedra, it seems appropriate to consider berlinite a crystal of PO_4 molecules which are linked via the interactions with the aluminium ions. The investigation of the equilibrium conditions adds further evidence to this picture of a crystal built up from tetrahedral units.

Using the equilibrium conditions we have adjusted the model parameters to the structural changes occurring with temperature. In the case of α-quartz, this procedure gives a very satisfactory description of the frequency spectrum up to the transition temperature. In berlinite the strong irregular variations of the bond lengths severely compromise all efforts to establish dependences of model parameters upon temperature.

Berlinite is not the only isotype of quartz; both crystals belong to a large family of binary and ternary compounds sharing a common structure (see Kosten and Arnold 1980, Bethke *et al* 1992). It is our aim to include these crystals in a future study. The main obstacle to date is the lack of reliable experimental data.

Although highly desirable, *ab initio* calculations for the lattice dynamics of berlinite are still unfeasible due to the large number of inequivalent ions in conjunction with a low-symmetry structure.

Acknowledgments

One of us, HS, would like to acknowledge the hospitality of the Institut Laue–Langevin including the permission to use its computer facilities. The calculations were carried out using a modified version of UNISOFT (Eckold *et al* 1987).

References

Averbuch-Pouchot M T 1993 *Z. Kristallogr.* **207** 111
Barron T H K, Huang C C and Pasternak A 1976 *J. Phys. C: Solid State Phys.* **9** 3925
Bethke J, Dolino G, Eckold G, Berge B, Vallade M, Zeyen C M E, Hahn T, Arnold H, Moussa F 1987 *Europhys. Lett.* **3** 207
Bethke J, Eckold G and Hahn Th 1992 *J. Phys.: Condens. Matter* **4** 5537
Binggeli N, Trouiller N, Martins J L, Chelikowsky J R 1991 *Phys. Rev.* B **44** 4771
Bond W L 1965 *J. Appl. Phys.* **36** 1674
Boyer L L 1974 *Phys. Rev.* B **9** 2684
Boyer L L and Fleury P A 1974 *Phys. Rev.* B **9** 2693
Boysen H, Dorner B, Frey F and Grimm H J 1980 *J. Phys. C: Solid State Phys.* **13** 6127
Camassel J, Goullet A and Pascual J 1988 *Phys. Rev.* B **38** 8419
Chelikowsky J R, King H E Jr, Trouiller N, Martins J L and Glinnemann J 1990 *Phys. Rev. Lett.* **65** 3309
Dove M T 1989 *Am. Mineral.* **74** 774
Eckold G, Stein-Arsic M and Weber H J 1987 *J. Appl. Cryst.* **20** 134
Elcombe M M 1967 *Proc. Phys. Soc* **91** 947
Gervais F and Piriou B 1975 *Phys. Rev.* B **11** 3944
Grimm H and Dorner B 1975 *J. Phys. Chem. Solids* **36** 407
Herzberg G 1945 *Molecular Spectra and Molecular Structure. II. Infrared and Raman Spectra of Polyatomic Molecules* (Princeton: Van Nostrand) p 167
Jayaraman A, Wood D L and Maines R G Sr 1987 *Phys. Rev.* B **35** 8316
Keating P N 1966 *Phys. Rev.* **145** 637
Kosten K and Arnold H 1980 *Z. Kristallogr.* **152** 119
Kruger M B and Jeanloz R 1990 *Science* **249** 647
Ng H N and Calvo C 1976 *Can. J. Phys.* **54** 638
Pantelides S T 1975 *Phys. Rev. Lett.* **35** 250
Pantelides S T and Harrison W A 1976 *Phys. Rev.* B **13** 2667
Posner A S, Perloff A and Diorio A F 1958 *Acta Crystallogr.* **11** 308
Schober H and Strauch D 1993 *J. Phys.: Condens. Matter* **5** 6165
Schober H, Strauch D, Nützel K and Dorner B 1993 *J. Phys.: Condens. Matter* **5** 6155
Schwarzenbach D 1966 *Z. Kristallogr.* **123** 161
Scott J F 1968 *Phys. Rev. Lett.* **21** 907
—— 1971 *Phys. Rev.* B **4** 1360
Shapiro S M, O'Shea D C and Cummins H Z 1967 *Phys. Rev. Lett.* **19** 361
Sidek H A A, Saunders G A, Hong W, Bin X, Jianru H 1987 *Phys. Rev.* B **36** 7612
Sinha S K 1973 *Crit. Rev. Solid State Sci.* **4** 281–93
Smith G S 1963 *Acta Crystallogr.* **16** 542
Strauch D and Dorner B 1993 *J. Phys.: Condens. Matter* **5** 6149
Wright A F and Lehmann M S 1981 *J. Solid State Chem.* **36** 371
Young R A 1962 *Defence Documentation Centre report* **AD 276 235**